Journal of Applied Fluid Mechanics, Vol. 16, No. 8, pp. 1574-1586, 2023.
Available online at www.jafmonline.net, ISSN 1735-3572, EISSN 1735-3645.
https://doi.org/10.47176/jafm.16.08.1745

Improving Thermal Performance of Rectangular Microchannel Heat Sinks using Porous Layer: CFD Simulation and Optimization

F. Montazeri [1], M. R. Tavakoli [2†], and M. R. Salimpour [2]

[1] *Mechanical Engineering Group, Pardis College, Isfahan University of Technology, Isfahan 8415683111, Iran*
[2] *Department of Mechanical Engineering, Isfahan University of Technology, Isfahan, 8415683111, Iran*

†*Corresponding Author Email: mrtavak@iut.ac.ir*

ABSTRACT

Microchannel heat sinks are very widely used due to their high heat transfer coefficients and low refrigerant requirements. Nevertheless, microchannel heat sinks still perform sub-optimally when it comes to thermal performance. Therefore, this paper investigates the individual and combined impacts of different characteristics of porous media on the thermal performance of microchannel. Four porosity values are considered: 0.8, 0.85, 0.9, and 0.95. The evaluation is based on three-dimensional computational fluid dynamics simulations. Due to the large number of degrees of freedom in this study, Constructal Theory and Design of Experiments are employed. In this study, the response surface type is Genetic Aggregation, while the Latin Hypercube Sampling algorithm is used for data sampling and Genetic algorithm is used for optimization. Combining porous layers with microchannel heat sinks reduces maximum temperatures about 3K. It is also observed that a lower maximum surface temperature is achieved in the cases with less porosity. Furthermore, the optimal geometry and size of the microchannels with porous layers are determined.

Article History

Received January 4, 2023
Revised March 14, 2023
Accepted April 3, 2023
Available online May 31, 2023

Keywords:

Heat transfer
Porous layer
Microchannel heat sinks
Constructal theory
Optimal geometry

1. INTRODUCTION

Microchannels are widely used in electronic cooling systems, space mission equipment, and heat exchangers. A microchannel heat sink is composed of a number of small channels with parallel and close fins on the heating surface. Tuckerman and Pease (1981), first proposed the concept of a microchannel heat sink. They developed an effective method for designing microchannel heat sinks in a laminar and fully developed flow. In this particular case, they found the optimal dimensions for a square-shaped silicon heat sink. Microchannels generally use liquid coolers with a higher heat transfer coefficient than gas coolers. Mahalingam (1985) experimented with air-cooled or water-cooled silicon heat sinks in 1985. According to his results, air cooled ducts had a thermal resistance of 0.7 cm^2.°C/W, while water cooled the ducts had a thermal resistance of 0.02 cm^2.°C/W. Through conductive heat transfer, the heat from the microchannel heat sink layer is transferred to the cooling fluid, which is then transferred by forced convection. Several factors can be considered in order to increase heat transfer from the solid part of the microchannel heat sink to the cooling fluid. Those factors include: Increasing the heat transfer surface by utilizing fins (Maji & Choubey, 2020), using a porous medium (Ghahremannezhad & Vafai, 2018), optimizing the design of the microchannel heat sink based on the thickness of the microchannels (Bello-Ochende et al., 2007), selecting a microchannel cross-section with the appropriate geometry (Salimpour et al., 2013), and using an appropriate arrangement to enter and exit the flow (Salimpour et al., 2019).

Peng et al. (1994) used an experimental method to determine the Reynolds number of the transition state in microchannels. Moreover, the Reynolds number of transition state decreases with decreasing channel dimensions. The thermal properties of fluid were examined by Peng and Peterson (1995) by varying the dimensions of rectangular microchannels. According to their findings, the channel undergoes a sudden change in thermophysical properties, which increases the Reynolds number as a result. In this study, it was found that laminar flow regimes convert to turbulent flow regimes at lower Reynolds numbers than conventional channels. Computational fluid dynamics were used by Wang et al. (2009) to study convection heat transfer in microchannels with negligible axial conductivity and compare the results with experimental results. The aim was to investigate

Nomenclature

t_{s1}	bottom thickness of solid	opt	optimum
t_{s2}	thickness of vertical solid	s	solid
t_{s3}	top thickness of solid	Re	Reynolds number
t_1	bottom thickness of porous	T	temperature
t_2	thickness of vertical porous	T_{in}	inlet temperature of coolant
t_3	top thickness of porous	T_o	outlet temperature of coolant
u	average streamwise velocity	T_{max}	maximum temperature in the heat sink
Greek symbols		Cp	specific heat
ϕ	volume fraction of solid material	C1	inertial resistance
ε	porosity of the porous medium	D_h	hydraulic diameter = $4A_c/P_c$
μ	dynamic viscosity	K	permeability of the porous medium
ρ_f	density of the fluid	L_x	width of the heat sink
ΔP	pressure drop between the channel inlet and outlet	L_y	height of the heat sink
Δx	thickness of the porous layer	L_z	length of the heat sink or channel length
Subscript		P	pressure
f	fluid	P_{out}	outlet pressure
in	inlet	$q^{"}$	heat flux applied to bottom surface
out	outlet		

the applicability of the Navier-Stokes equations in microchannels. According to Yilmaz et al. (2000), there is a minimum pressure drop at which maximum heat transfer occurs. For forced convection heat transfer in laminar flows in channels with different shapes, this study investigated the maximum heat transfer and optimal dimensions for a given pressure drop. Salimpour et al. (2011) investigated heat transfer in an array of circular and non-circular channels in a constant volume and pressure drop. Furthermore, in another study (2013), they showed that there is an optimal hydraulic diameter for microchannel heat sinks that maximizes thermal conductivity. They examined microchannels with different cross-sectional areas, determined the optimal dimensions for having the highest heat transfer in a constant volume, and discovered that rectangular geometry in a given volume has the best structure for a specific pressure drop among various geometries.

Using a porous medium can increase the heat transfer coefficient and reduce the maximum wall temperature of the microchannel heat sink. By placing porous layers inside microchannels, the surface-to-volume ratio and cooling fluid velocity are enhanced, resulting in improved heat transfer. Aluminum, copper, and silver are thermally conductive materials that can be used as a porous medium. On the other hand, fluid passing through the porous matrix experiences a significant pressure drop. The porous medium parameters in a heat exchanger must be optimized according to the fluid pressure drop at the design stage to achieve maximum heat transfer. An experimental and numerical study by Bogdan & Abdulmajeed (2004) demonstrated that using different porous media inside a tube with uniform heat flux increased the rate of heat transfer between the tube and the airflow. A porous heat sink system was used by Wan et al. (2011) to control and improve heat transfer in high-power LED components. As the fluid velocity increases, the average heat transfer coefficient increases, as does using a porous heat sink system, which reduces the temperature of the heating surface, which is essential for LEDs. A rectangular channel with porous layers periodically placed on its upper and lower walls was investigated by Yang and Hwang (2003). In their study, they found that porous channels have a lower friction factor, which improves heat transfer, than smooth channels. It was concluded by Ould-Amer et al. (1998) that adding porous material to heat-generating blocks would increase the Nusselt number and decrease the block's maximum temperature. Hung et al. (2013a) investigated the thermal performance of microchannel heat sinks with porous layers in various shapes and concluded that increasing the Reynolds number increased the heat transfer coefficient. Meanwhile, porous layers with rectangular distributions show the greatest improvement in heat transfer coefficient at high Reynolds numbers. Another study by Hung et al. (2013b) showed that in microchannels with porous media, the average Nusselt number is higher than in microchannels without it. In a microchannel with a porous medium, there is a significant pressure drop between the inlet and outlet, but this pressure drop can be reduced by increasing the outlet's width or height enlargement ratio. Ghahremannezhad and Vafai (2018), by using porous materials with different thicknesses in microchannel heat sinks, concluded that porous materials have the necessary potential to improve the thermal and hydraulic performance of microchannels. Moreover, they showed that the correct thickness of the porous material and the solid part of the microchannel heat sink can reduce the required heat resistance and pump power.

Most studies have shown that porous structures improve the performance of microchannel heat sinks. However, the thermal performance of microchannels in the presence of porous materials with a constant volume has not been investigated so far. It is significant to note that in the study conducted by Ghahremannezhad and Vafai (2018), porous layers were examined in two directions separately without considering fixed conditions. The volume of the solid surface of the

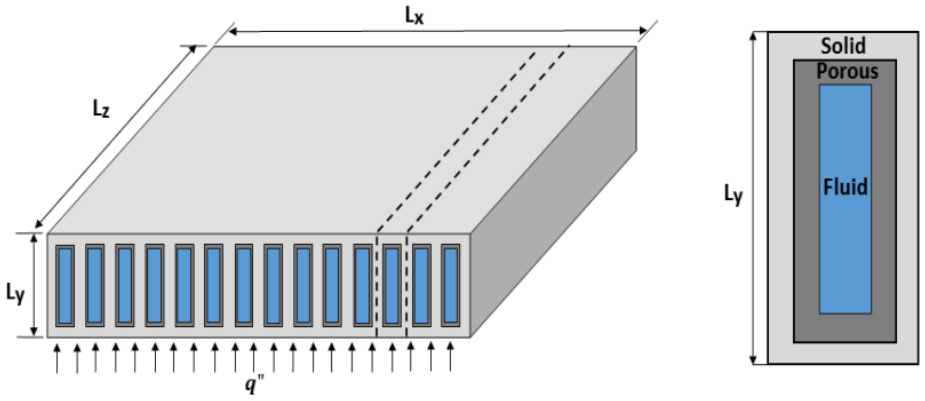

Fig. 1. Schematic image of the microchannel heat sink and computational domain.

microchannel also varies. In the present research, the effect of using porous materials is analyzed simultaneously in all directions to determine the thermal performance of microchannels under a constant volume. Moreover, this study aims to determine the optimal arrangement of porous materials and the solid part of the microchannel in order to improve the performance of microchannel heat sinks. The microchannel heat sink is described in Section 2. The numerical procedure is presented in Section 3. The grid independency for CFD simulations is presented in Section 4. The results of the optimization are provided in Section 5. And the main conclusions are presented in Section 6.

2. DESCRIPTION OF THE PROBLEM

This research investigates the thermal performance of microchannel heat sinks with rectangular cross-sections when layers of porous material are placed inside them. The geometrical characteristics of the porous layers and the microchannels are optimized to minimize the total thermal resistance and therefore increase heat transfer. This will lead to the lowest possible maximum wall temperature.

As shown in (Fig. 1), a uniform heat flux is applied to the lower surface of the microchannel heat sink, and the upper surface is considered adiabatic. Inside the microchannel, water flows as a cooling fluid. Due to the small dimensions of the microchannel (H = 100 μm, Ly = 800 μm, Lz = 10 mm) and the short entrance length (1.19 mm) compared to the length of the microchannel, a laminar, incompressible, and fully developed fluid flow is assumed. Continuity, momentum, and energy equations are solved numerically using the finite volume method. The microchannel and its surrounding solid walls are considered as a computational domain due to geometric symmetry. A combination of convective and conductive heat transfer occurs in this volume. Because the channel length is larger than its width, Local Thermal Equilibrium (LTE) is assumed between the solid and the coolant through the porous domains (Vafai & Tien 1981; Vafai 1984; Vafai & Thiyagaraja 1987; Hsu & Cheng 1990; Amiri et al. 1995; Alazmi & Vafai 2001).

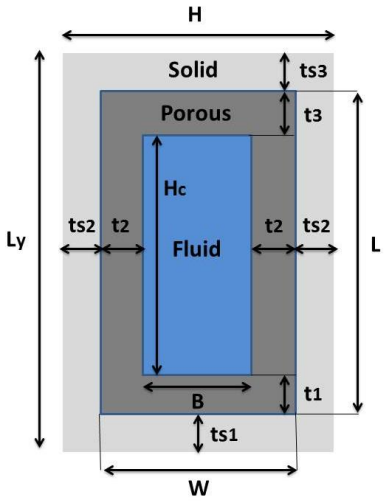

Fig. 2. Geometric parameters of the microchannel heat sink with porous layers.

Initially, the volume of the porous material is considered a fixed constraint. The optimal thickness of microchannel walls without porous material has already been identified by Bello-Ochende et al. (2007). So, the first objective of this research is to determine the thickness of porous material in each wall of the same microchannel that is shown in (Fig. 2). Due to the symmetry and constant thickness of the solid part in this step, the degrees of freedom are only t_1/t_2 and t_1/t_3. Using Constructal Theory, the optimal thicknesses would be determined under porosity variations and constant pressure drops.

In the second step, the solid part of the microchannel heat sink and the porous material volume are considered fixed. Due to the fact that none of the thicknesses are known at this stage, the goal of this step is to determine the optimal thickness of microchannel walls and porous material by using Design of Experiment and data-driven optimization under various values of porosity and constant pressure drop (Fig. 2). The final step will determine the optimal porosity for the porous material based on the porosity of porous materials available on the market. In this study, six parameters are considered as inputs or independent

parameters: the thickness of the porous layer and the solid part of the microchannel heat sink (t_1, t_2, t_3, t_{s1}, t_{s2}, t_{s3}). And one parameter, the maximum temperature of the microchannel surface, is considered the output or dependent parameter.

2.1. The Governing Equations of the Problem

The present study investigates numerically the flow and heat transfer in a microchannel in which layers of porous medium have been added. The governing equations are discussed in this section. A large number of studies have been conducted on flow and heat transfer in porous media since the nineteenth century. The first attempt was made by Darcy in 1956, when he introduced his famous Darcy law. According to this law, the pressure drop within a porous medium can be expressed as follows:

$$-\frac{dp}{dx} = \frac{\mu}{k}u \tag{1}$$

Where $\frac{dP}{dx}$ is the pressure gradient, u is the average streamwise velocity, μ is the dynamic viscosity of the fluid, and k is the permeability of the porous medium, a measure of the resistance that a fluid faces as it passes through a porous medium. Several studies have shown that adding a porous medium to a channel increases the pressure drop significantly (Bogdan & Abdulmajeed 2004; Hetsroni et al., 2006; Hung et al., 2013b; Ghahremannezhad & Vafai, 2018). There has been demonstrated that for all studied environments, the axial pressure drop is the sum of two expressions (Hetsroni et al., 2006; Jiang & Lu, 2006), one with a linear contribution from viscosity (viscosity contribution) and one with a quadratic contribution from inertia (inertia contribution).

$$-\frac{dp}{dx} = \frac{\mu}{k}u + \frac{c_F\,\rho}{\sqrt{k}}u^2 \tag{2}$$

In the above relation, c_F is the inertia coefficient; ρ the density of the fluid; dP/dx the pressure gradient; u the average velocity; μ the dynamic viscosity of the fluid and k is the permeability of the porous medium. The porous medium is assumed to be rigid, homogeneous, isotropic, and fully saturated with fluid. It is assumed that fluid flow is incompressible, laminar, and steady. There is no gravity effect or radiation heat transfer inside the channels; the thermophysical properties of the materials are constant. In porous media, flow and heat transfer characteristics are calculated using volume-averaged techniques and the Brinkman–Darcy–Forchheimer model. According to the above assumptions, the equations governing porous media are as follows (Vafai & Tien 1981):

Continuity equation:

$$\nabla.\left(\varepsilon\rho_f V\right) = 0 \tag{3}$$

Table 1 Thermal properties of cooling fluid, solid part, and porous layers.

Materials	ρ (kg/m^3)	C_p (J/kg.K)	k (W/m.K)
Water	998	4182	0.598
Silicon	2330	712	148
Aluminium	2702	903	237

Where ρ_f is the density of the fluid, and V is the velocity vector of the fluid.

Momentum equation:

$$\frac{\rho_f}{\varepsilon^2}(V.\nabla)V = -\nabla_p - \left(\frac{\mu_f}{k_p} + \frac{\rho_f C}{\sqrt{k_p}}|V|\right)V + \frac{\mu_f}{\varepsilon}\nabla^2 V \tag{4}$$

Where ε is the porosity of the porous medium; k_p is the permeability; C is Forchheimer constant, and μ_f is the viscosity of the fluid.

Energy equation:

$$(\rho C)_e(V.\nabla T) = k_e\nabla^2 T \tag{5}$$

Where T is temperature, $k_e = \varepsilon k_f + (1-\varepsilon)k_s$ and $(\rho C)_e = \varepsilon\rho_f C_f + (1-\varepsilon)\rho_s C_s$ are the effective thermal conductivity and the heat capacity of the porous media, respectively.

3. NUMERICAL PROCEDURE

In the present research, the commercial CFD code ANSYS Fluent 2019 is used to perform the simulations. The finite volume method is used to solve the continuity, momentum, and energy equations. The SIMPLE algorithm is employed to solve the pressure–velocity coupling, while a second-order upwind scheme is invoked to discretize the equations. The convergence is assumed to reach when the residuals of continuity, momentum, and energy reach 10^{-6}. Microchannel heat sinks with rectangular cross-sections and 10 mm length are considered for this study. In the opening of the microchannel, layers of porous materials made of aluminum are placed on silicon walls. Water is used as the coolant in this study. All materials used in this study are listed in (Table 1).

3.1 Computational Domain

In (Fig. 3), the computational domain and grid for the microchannel heat sink can be seen. On porous layers and near heat sources where velocity and temperature gradients are more significant, the discretization grid is finer.

3.2 Boundary Conditions

The boundary conditions for the computational domain are as follows, which are shown schematically in (Fig. 4):

- The inlet temperature of the fluid is 20 ºC and the pressure drop between the inlet and outlet of the channel is constant and 50 KPa (point 1).

- The pressure is constant and atmospheric, at the microchannel outlet (point 2).

- Symmetry is established in the side walls of the microchannel.

- The lower wall of the microchannel (surface 5) is heated with constant and uniform heat flux.

- The upper wall of the microchannel (surface 6) is insulated and adiabatic.

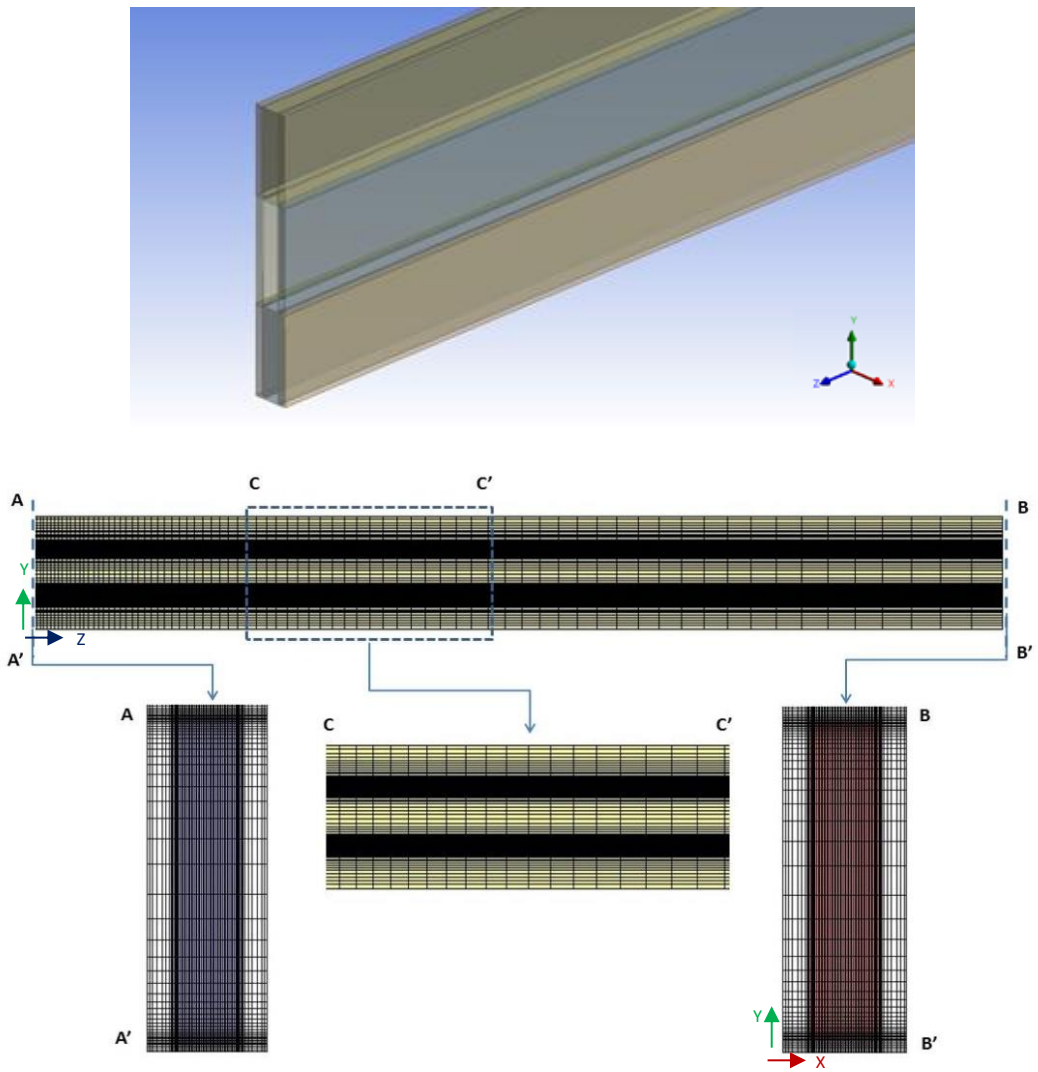

Fig. 3. Computational domain and grid of the microchannel heat sink with porous layers.

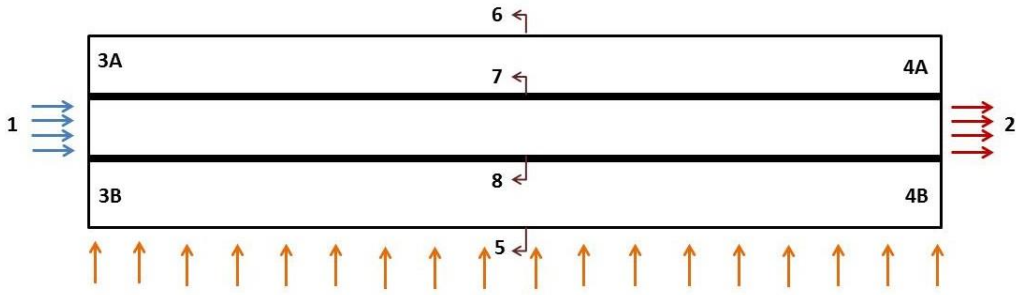

Fig. 4. Schematic of boundary condition.

Table 2. The experimental data of Hetsroni et al. (2006).

U (m/s)	ΔP (Pa)
11.48	35000
20.88	112500
28.18	206000

3.3 Inertial and Viscous Resistance

In the equations related to the porous medium, there are two parameters of inertial resistance (C1) and viscous resistance (1/k) that we need to have for the investigation. For this purpose, the data in Hetsroni et al (2006), which can be seen in (Table 2), have been used to calculate the inertial and viscous resistance.

Finally, using the following equations, the values of C1 and 1/k are obtained:

$$\Delta P = aU^2 + bU \tag{6}$$

$$\frac{1}{K} = \frac{b}{\mu \Delta x_i} \tag{7}$$

$$C_1 = \frac{2a}{\rho \Delta x_i} \tag{8}$$

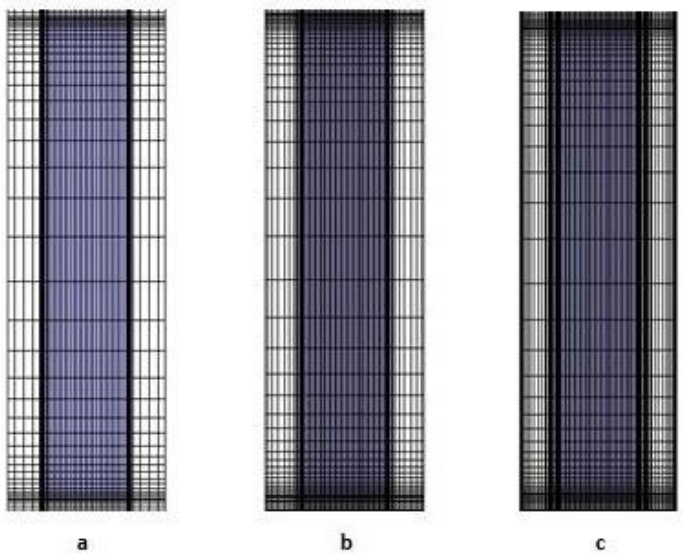

Fig. 5. Computational grids (a) Coarse grid (b) basic grid (c) fine grid.

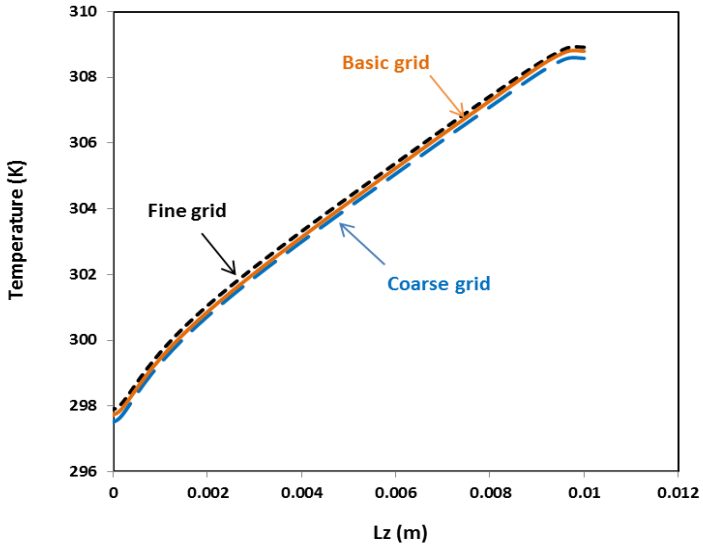

Fig. 6. Results for temperature changes along a horizontal line on the lower surface for three grids.

Table 3. Number of cells and maximum temperature associated with different grids

Mesh	Number of cells	T_{max} (K)
Coarse	415245	308.744
Basic	830280	308.809
Fine	1798200	308.801

Where μ and ρ are the viscosity and density of the fluid, respectively. Constants a and b are the coefficients of the equation obtained from the pressure drop diagram, and Δx is the thickness of the porous layer.

4. GRID INDEPENDENCY

In this research, three grids with different cell numbers have been produced. These three grids, which we call Coarse, Basic and Fine, have 415245, 830280 and 1798200 cells, respectively. They can be seen in (Fig. 5).

The analysis is based on the above three grids and performed for the reference state, in which the porous thickness is five micrometers in all directions, and almost similar results were obtained (As shown in Table 3). The deviation between the coarse and the basic grids and the basic and fine grids are 0.021% and 0.003%, respectively indicating the fact that the solution process is independent of the type of grid and the number of cells.

Furthermore, temperature changes along a horizontal line on the lower surface for three grids are shown in (Fig. 6). The average deviation between the coarse and the basic grids and the basic and fine grids are 0.14% and 0.13%, respectively. This indicates that the CFD results do not significantly change by refining the grid. Therefore, the basic grid is used for all simulations.

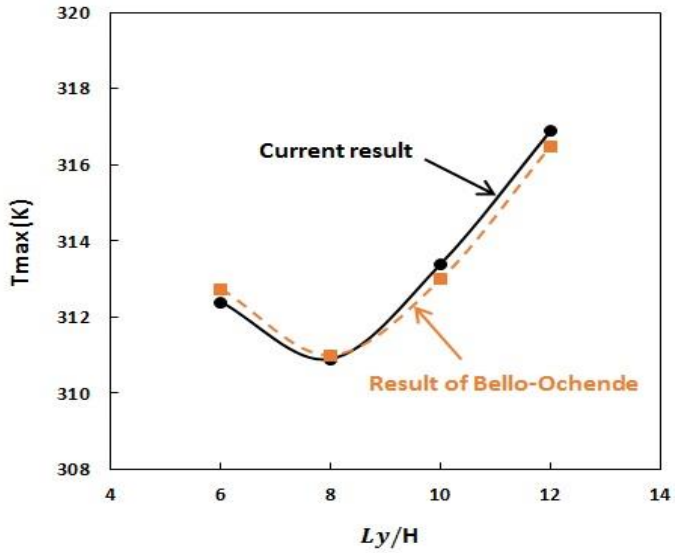

Fig. 7. Maximum temperature in Bello-Ochende et al. (2007) and the present research (Ø = 0.8, ΔP = 50 kPa)

Table 4. Dimensions used in the first step with $t_1/t_3 = 1$

	t_2 (μm)	t_1 (μm)	t_3 (μm)	t_{s1} (μm)	t_{s2} (μm)	t_{s3} (μm)
A_1	2	20.536	20.536	250	20	250
A_2	2.5	18.182	18.182	250	20	250
A_3	3	15.741	15.741	250	20	250
A_4	3.5	13.208	13.208	250	20	250
A_5	4	10.577	10.577	250	20	250
A_6	4.5	7.843	7.843	250	20	250
A_7	5	5	5	250	20	250
A_8	5.5	2.041	2.041	250	20	250

4.1 Comparison with Other Studies

In this section, the accuracy and ability of numerical methods are examined by comparing the results of previous numerical work with the results of current work. A study published by Bello-Ochende et al. (2007) was used for this purpose. This paper evaluates the performance of a rectangular microchannel heat sink. As it is clear from the results of (Fig. 7), a fairly good agreement between the maximum temperatures obtained in this research and in the mentioned article is achieved.

5. RESULTS AND DISCUSSION

There are two stages in this research, as previously mentioned. As a first step, the Constructal Theory is used to determine the thickness of the porous layers. In the second stage, Design of Experiment (DOE) has been used because of the complexity and a high degree of freedom.

5.1 Constructal Theory

The exact dimensions of the microchannel heat sink with the rectangular cross-section without porous layers have been used in this study since Bello-Ochende et al. (2007) determined the optimal dimensions. Aluminum porous material is then used to fill 20% of the microchannel internal opening. At this stage, the volume of porous material is constant and the dimensions have changed to the extent that this condition has been met. At this stage, only the thicknesses of the porous layers are examined, as shown in (Table 4). According to the method of Constructal Theory, at first, the ratio of t_1/t_3 is considered equal to one, and then, according to the condition of constant volume of porous materials, change the thickness t_2 to get the best thickness, which is related to minimizing maximum surface temperature.

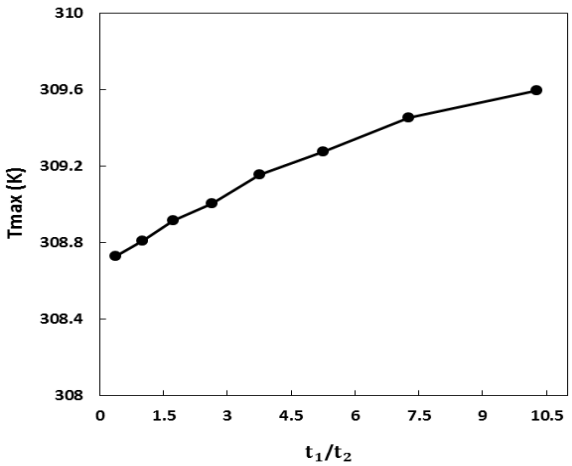

Fig. 8. Effect of thickness t_2 on maximum temperature.

Figure 8 shows the effect of the porous thickness on the right and left sides of the microchannel opening on the maximum surface temperature. From the result of this figure and (Table 4), we can find the best thickness for t_2,

Table 5. Dimensions used in the first step with t_2 = 5.5 µm

	t_2 (μm)	t_3 (μm)	t_1 (μm)	t_{s1} (μm)	t_{s2} (μm)	t_{s3} (μm)
B_1	5.5	1	3.082	250	20	250
B_2	5.5	1.5	2.582	250	20	250
B_3	5.5	2	2.082	250	20	250
B_4	5.5	2.5	1.582	250	20	250
B_5	5.5	3	1.082	250	20	250
B_6	5.5	3.5	0.582	250	20	250

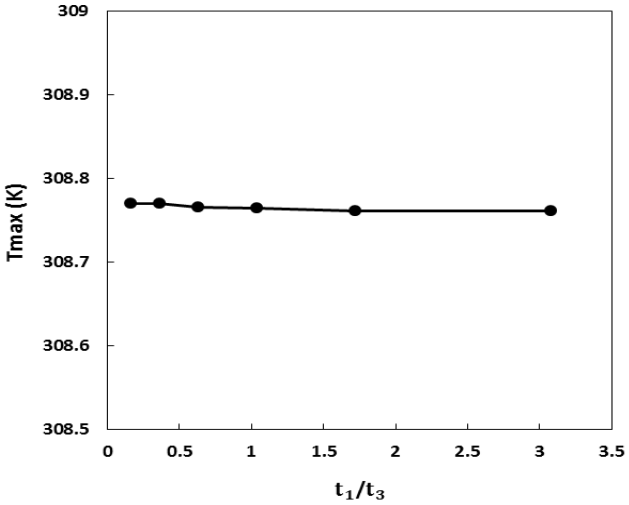

Fig. 9. Effect of thickness t_1 and t_3 on maximum temperature.

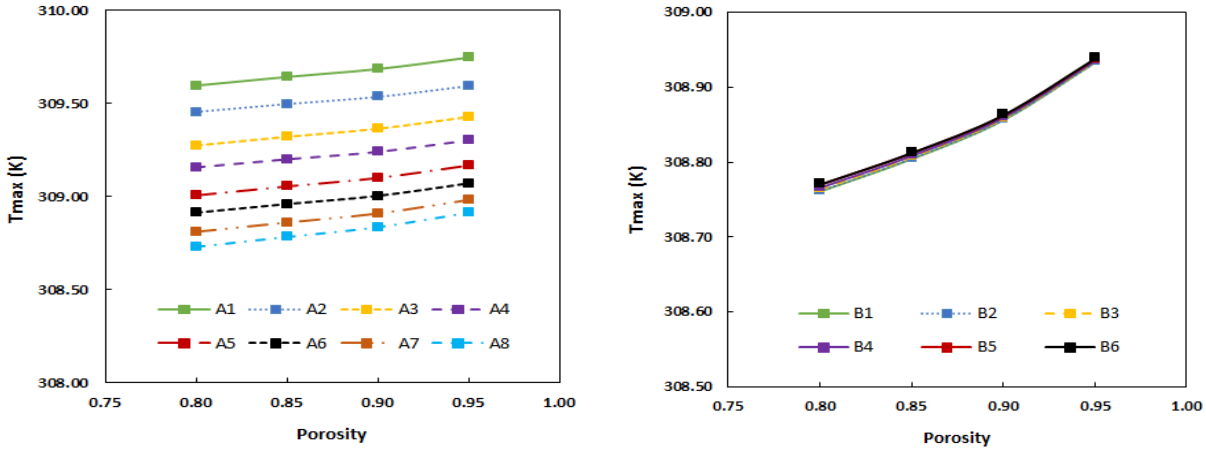

(a) (b)

Fig. 10. Effect of porosity on maximum temperature: (a) dimensions in Table 4, (b) dimensions in Table 5.

which is 5.5 µm, corresponding to the point where the maximum temperature is the minimum.

Then, by placing the constant value obtained for the thickness t_2, changing the thickness of the porous layer at the top of the microchannel opening (t_3), and considering the constant volume of the porous layer, the thickness of the lower part (t_1) is calculated. (Table 5) shows the range of changes for the mentioned parameters.

As shown in (Fig. 9), when the thickness of the solid part of the microchannel heat sink is constant and only the porous layers are changing, the thickness of the porous layer at the top and bottom of the microchannel opening has little effect on the maximum temperature that is negligible. The maximum temperature is then investigated in relation to the porosity of the porous layers. Thus, all geometric dimensions in (Table 4) and (Table 5) are solved for porosity values of 0.8, 0.85, 0.9, and 0.95. Figure 10 illustrates the results. The maximum temperature increases with a gentle slope as the porosity increases, so the best porosity value is 0.8. Moreover, it should be noted that in (Fig. 10.a), all the values for porosity correspond to point A_8, has the greatest impact on improving heat transfer, and as it gets to point A_1, the maximum temperature has increased. It can be interpreted that the increment in t_1 makes the thermal resistance higher and increases the maximum temperature. In other words, moving the channel toward the heated bottom

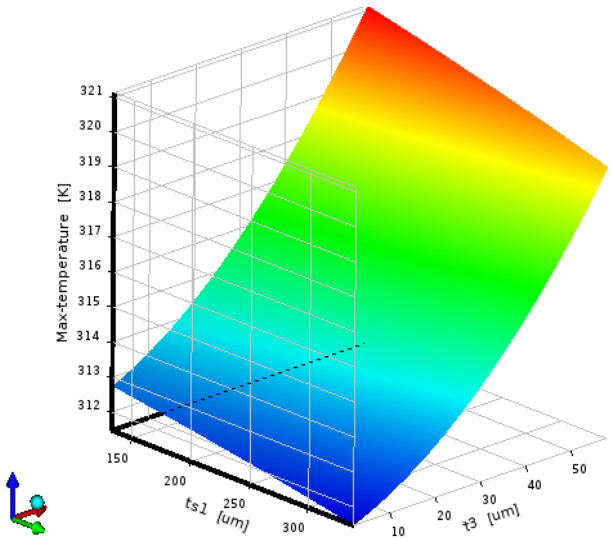

Fig. 11. Response Surface.

surface increases the opportunity for heat removal, because in the lower region, temperatures are higher, thus, cooling rate would be improved. And as shown in (Fig. 10.b), all dimensions in (Table 5) behave similarly but they show the same result.

5.2 Design of Experiment

In the present study, due to the large number of degrees of freedom, data-driven optimization is used. Data-driven optimization generally consists of three steps: sampling, metamodeling and optimization. Data-driven models are statistical models developed based on a limited number of simulations to predict the output results of simulations yet to be performed (Kaseb & Montazeri, 2022). In this study, the response surface type is Genetic Aggregation, while the Latin Hypercube Sampling algorithm is used for data sampling and Genetic algorithm is used for optimization. In this section, besides the thickness of the porous layers, the thickness of the solid part of the microchannel heat sink also changes. All these changes are made under the condition that the volume of the porous material and the solid part of the microchannel are constant. It is possible to investigate the simultaneous effects of all input parameters on the output parameter using this method. The solid part of the microchannel and the porous layers should have the proper thickness to minimize the maximum surface temperature. As input parameters, all thicknesses in (Fig. 2) are defined and the minimum and maximum values of them are determined according to the constant volume. This research only produces the maximum surface temperature of microchannels as an output parameter. In this case, the input parameters and the constant volume condition result in 70 points called Design Points with different dimensions. Using the relationship between input and output parameters, a response surface is defined after solving and finding the output parameter. Figure 11 shows how input parameters affect output parameters in relation to this surface. In order to improve the accuracy of this surface, 33 points are added called Refinement Points. When these points are solved, the error in determining this response surface is reduced. To verify the accuracy of this surface for the points not used in its construction, 23 other points are defined as Verification Points. Additionally, (Fig. 12) compares the calculated maximum temperatures based on CFD with the estimated maximum temperatures using the response surface. The results are very close and there is not much difference between them. So, it is obvious that the answer is reliable.

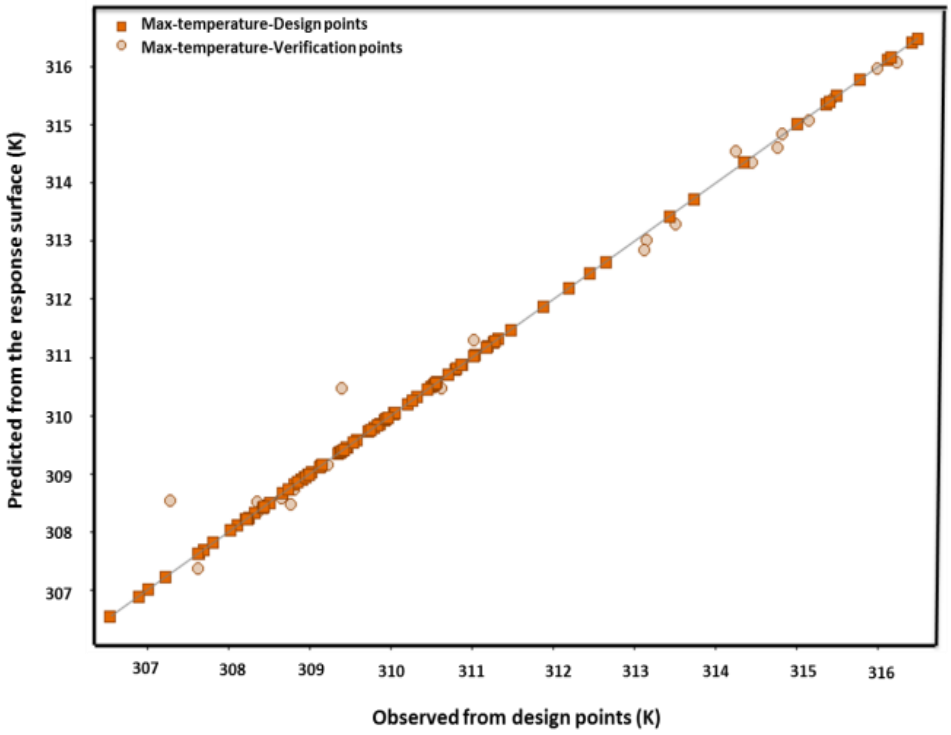

Fig. 12. Comparison of CFD results and the results of the response surface.

Table 6 Optimal dimensions for porous layers and solid part of the microchannel heat sink.

	t_1 (μm)	t_2 (μm)	t_3 (μm)	t_{s1} (μm)	t_{s2} (μm)	t_{s3} (μm)
DP_1	9.372	5.2257	16.823	133.95	11.077	280.94
DP_2	10.186	5.2436	18.403	136.94	11.028	297.43
DP_3	8.8338	5.4241	20.453	138.65	11.144	307.34
DP_4	11.474	5.2524	18.268	135.28	11.167	300.95
DP_5	12.398	5.4876	17.104	136.67	11.159	300.35

Table 7 Maximum temperature obtained from the simulation and optimization for the optimal dimensions.

t_1 (μm)	t_2 (μm)	t_3 (μm)	t_{s1} (μm)	t_{s2} (μm)	t_{s3} (μm)	T_{max} (K) Optimization	T_{max} (K) Real
9.372	5.2257	16.823	133.95	11.077	280.94	306.14	306.52
10.186	5.2436	18.403	136.94	11.028	297.43	306.15	306.54
8.8338	5.4241	20.453	138.65	11.144	307.34	306.17	306.54
11.474	5.2524	18.268	135.28	11.167	300.95	306.17	306.55
12.398	5.4876	17.104	136.67	11.159	300.35	306.17	306.49

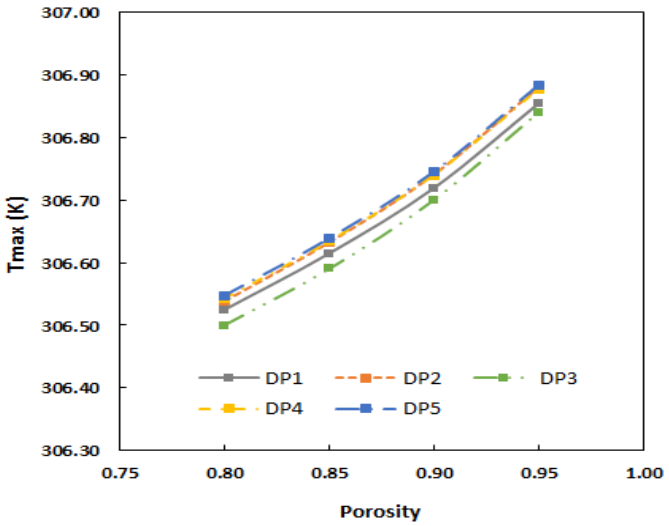

Fig. 13. Effect of porosity on the maximum surface temperature: dimensions in Table 6.

After the above steps, the minimum and maximal values are specified for each parameter according to the constant volume of the porous layers and the solid part of the microchannel. Using the state of minimizing maximum surface temperature as well, the five candidates with the most optimal dimensions are shown in (Table 6). To verify the accuracy of the results, simulations have been performed for the dimensions derived from this method. Afterwards, the maximum surface temperature of the optimization method was compared with the maximum surface temperature of the solution. (Table 7) shows slightly different results and confirms the results accuracy.

In the last step of this research, the dimensions obtained from the optimization method shown in (Table 6) were solved for different values of porosity. The results are shown in (Fig. 13). According to the behavior of each graph, the maximum temperature increases with increasing porosity. The reason is that at higher porosities thermal resistance increases. Therefore, the appropriate porosity in this study is 0.8, which corresponds to the minimum temperature. As expected, this is the same result as the Constructal Theory's optimization. Finally, the contours of temperature along the microchannel heat sink for four different models are shown. They demonstrate how layers of porous materials can improve heat transfer and reduce the maximum surface temperature. For all cases, temperature increases from inlet to the outlet and the maximum temperature occurs at the bottom surface of the microchannel heat sink, where the coolant fluid exits the channel. In (Fig. 14), there is no layer of porous material inside the microchannel heat sink. At the bottom of the outlet, the maximum surface temperature is 310K. (Fig. 15) shows a porous material filling the microchannel opening. It is evident that the maximum surface temperature has increased. As a result, it shows that the complete filling of the channel opening with porous material does not only improve heat transfer, but can actually increase surface temperatures. In (Fig. 16), the inner walls of the microchannel are covered with layers of porous material with a thickness of 5μm in all directions, and based on the temperature distribution, it is apparent that heat transfer is improved and maximum surface temperature is reduced. In (Fig. 17), the solid part of the

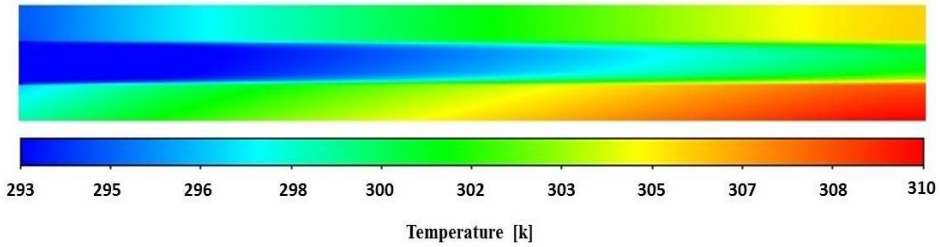

Fig. 14. Contour of temperature for the microchannel heat sink without porous material.

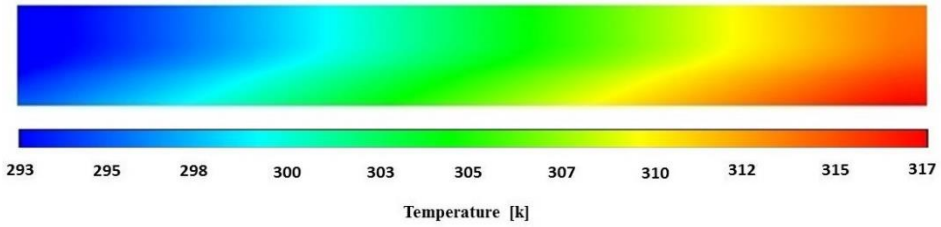

Fig. 15. Contour of temperature for the microchannel heat sink filled with the porous material.

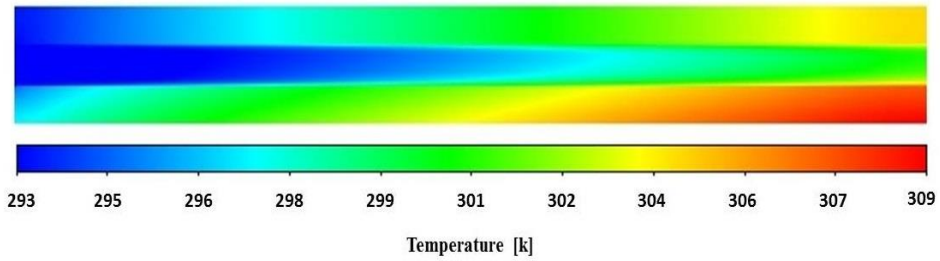

Fig. 16. Contour of temperature in the reference state (porous layers with a thickness of 5µm in all directions).

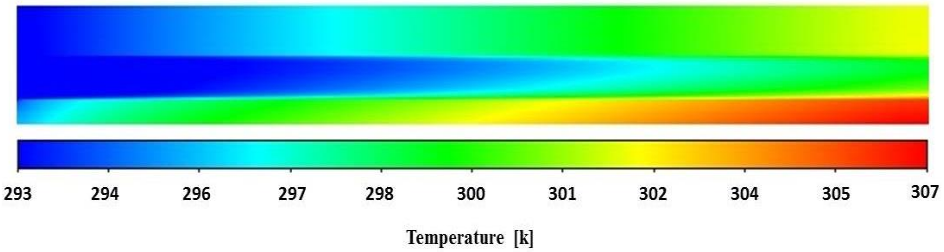

Fig. 17. Contour of temperature for the microchannel heat sink in the final optimal state.

microchannel as well as the porous layers is optimized based on the results obtained. A minimum temperature is evident in this case, which is the primary purpose of the study.

6. CONCLUSIONS

The purpose of this numerical study is to investigate the potential of porous inserts to enhance heat transfer in microchannels heated with a constant and uniform heat flux and cooled by water flowing inside the channels. In this study, porous layers in a rectangular microchannel heat sink were demonstrated to be an effective method of enhancing heat transfer. As a result, the following conclusions can be drawn:

(1) A carefully selected solid and porous thickness based on an optimization study can reduce thermal resistance and increase heat transfer. Thus, a lower maximum temperature will be achieved.

(2) Microchannel heat sinks have an optimal porous thickness that will have the highest total heat transfer coefficient.

(3) In the optimal state, the porous and solid parts of the microchannel heat sink in the lower part of the channel have a thinner thickness than the other walls. In this way, the points that receive heat will have maximum access to the cooling fluid, and heat transfer will be increased.

(4) Thermal resistance increases with increasing porosity. As a result, heat transfer will be reduced and the maximum temperature will be higher.

(5) Based on (Fig. 10) and (Fig. 13), the effect of porosity is stronger when the thickness of the porous layer is larger.

CONFLICT OF INTEREST

The authors declare that they have no competing interests.

AUTHOR CONTRIBUTION

F. Montazeri: conceptualization; data collection; visualization; writing the original draft. M. R. Tavakoli: conceptualization; supervision writing; review and editing. M. R. Salimpour: review and editing.

REFERENCES

Alazmi, B., & Vafai, K. (2001). Analysis of fluid flow and heat transfer interfacial conditions between a porous medium and a fluid layer. *International Journal of Heat and Mass Transfe*r 44, 1735–1749. https://doi.org/10.1016/S0017-9310(00)00217-9.

Amiri, A., Vafai, K., & Kuzay, T. M. (1995). Effect of boundary conditions on non-darcian heat transfer through porous media and experimental comparisons, Numer. *Heat Transfer Journal Part A*, 27, 651–664. https://doi.org/10.1080/10407789508913724

Bello-Ochende, T., Liebenberg, L., & Meyer, J. P. (2007). Constructal cooling channels for micro-channel heat sinks. *International Journal of Heat and Mass Transfer*, 50, 4141–4150. https://doi.org/10.1016/j.ijheatmasstransfer.2007.02.019

Bogdan, I. P. & A. A. Mohamad (2004). An experimental and numerical study on heat transfer enhancement for gas heat exchangers fitted with porous media. *International Journal of Heat and Mass Transfer*. 47, 4939–4952. https://doi.org/10.1016/j.ijheatmasstransfer.2004.06.014

Ghahremannezhad, A., & Vafai, K. (2018). Thermal and hydraulic performance enhancement of microchannel heat sinks utilizing porous substrates. *International Journal of Heat and Mass Transfer*. 122, 1313–1326. https://doi.org/10.1016/j.ijheatmasstransfer.2018.02.024

Hetsroni, G., Gurevich, M., & Rozenblit, R. (2006). Sintered porous medium heat sink for cooling of high-power mini-devices. *International Journal of Heat and Fluid Flow*, 27, 259–266. https://doi.org/10.1016/j.ijheatfluidflow.2005.08.005

Hsu, C. T., & Cheng, P. (1990). Thermal dispersion in a porous medium. *International Journal of Heat and Mass Transfe*r, 33, 1587–1597. https://doi.org/10.1016/0017-9310(90)90015-M

Hung, T. C., Huang, Y. X., & Yan, W. M. (2013a). Thermal performance analysis of porous-microchannel heat sinks with different configuration designs. *International Journal of Heat and Mass Transfer*, 66, 235–243. https://doi.org/10.1016/j.ijheatmasstransfer.2013.07.019

Hung, T. C., Huang, Y. X., & Yan, W. M. (2013b). Thermal performance of porous microchannel heat sink: Effects of enlarging channel outlet. *International Communications in Heat and Mass Transfer*, 48, 86–92. https://doi.org/10.1016/j.icheatmasstransfer.2013.08.001

Jiang, P. X., & Lu, X. C. (2006). Numerical simulation of fluid flow and convection heat transfer in sintered porous channels. *International Journal of Heat and Mass Transfer*, 49, 1685–1695. https://doi.org/10.1016/j.ijheatmasstransfer.2005.10.026

Kaseb, Z., & Montazeri, H. (2022). Data-driven optimization of building-integrated ducted openings for wind energy harvesting: Sensitivity analysis of metamodels. *Energy*, 258, 124814. https://doi.org/10.1016/j.energy.2022.124814

Mahalingam, M (1985). Thermal management in semiconductor device packaging. *Proceedings of the IEEE*, 73, 1396–1404. https://doi.org/10.1109/PROC.1985.13300

Maji, A., & Choubey, G. (2020). Improvement of heat transfer through fins: A brief review of recent developments. *Heat Transfer*, 49, 1658-1685. https://doi.org/10.1002/htj.21684

Ould-Amer, Y., Chikh, S., Bouhadef, K., & Lauriat, G. (1998). Forced convection cooling enhancement by use of porous materials. *International Journal of Heat and Fluid Flow*, 19, 251–258. https://doi.org/10.1016/S0142-727X(98)00004-6

Peng, X. F., Peterson, G. P., & Wang, B. X. (1994). Heat Transfer Characteristics of Water Flowing Through Microchannels. *Experimental Heat Transfer*, 7, 265–283. https://doi.org/10.1080/08916159408946485

Peng, X. F., & Peterson, G. P. (1995). The effect of thermofluid and geometrical parameters on convection of liquids through rectangular microchannels. *International Journal of Heat and Mass Transfer*, 38, 755–758. https://doi.org/10.1016/0017-9310(95)93010-F

Salimpour, M. R., Sharifhasan, M., & Shirani, E. (2011). Constructal optimization of the geometry of an array of micro-channels. *International Communications in Heat and*

Mass Transfer, 38, 93–99. https://doi.org/10.1016/j.icheatmasstransfer.2010.10.008

Salimpour, M. R., Sharifhasan, M., & Shirani, E. (2013). Constructal optimization of microchannel heat sinks with noncircular cross sections. *Heat Transfer Engineering*, 34, 863–874. https://doi.org/10.1080/01457632.2012.746552

Salimpour, M. R., Al-Sammarraie, A., Forouzandeh, A., & Farzaneh, M. (2019). Constructal Design of Circular Multilayer Microchannel Heat Sinks. *Journal of Thermal Science and Engineering Applications*, 11, 011001-10. https://doi.org/10.1115/1.4041196

Tuckerman, D. B., & Pease, R. F. W. (1981). High-performance heat sinking for VLSI. *IEEE Electron Device Letters.* 2, 126–129. https://doi.org/10.1109/EDL.1981.25367

Vafai, K., & Tien, C. L. (1981). Boundary and inertia effects on flow and heat transfer in porous media. *International Journal of Heat and Mass Transfe*r, 24, 195–203. https://doi.org/10.1016/0017-9310(81)90027-2

Vafai, K. (1984). Convective flow and heat transfer in variable porosity media. *Journal of Fluid Mechanics* 25, 233–259. https://doi.org/10.1017/S002211208400207X

Vafai, K., & Thiyagaraja, R. (1987). Analysis of flow and heat transfer at the interface region of a porous medium. *International Journal of Heat and Mass Transfe*r 30, 1391–1405. https://doi.org/10.1016/0017-9310(87)90171-2

Wan, Z. M., Liu, J., Su, K. L., Hu, X. H., & M, S. S. (2011). Flow and heat transfer in porous micro heat sink for thermal management of high power LEDs. *Microelectronics Journal*, 42, 632–637. https://doi.org/10.1016/j.mejo.2011.03.009

Wang, G., Hao, L., & Cheng, P. (2009). An experimental and numerical study of forced convection in a microchannel with negligible axial heat conduction. *International Journal of Heat and Mass Transfer*, 52, 1070–1074. https://doi.org/10.1016/j.ijheatmasstransfer.2008.06.038

Yang, Y. T., & Hwang, C. Z. (2003). Calculation of turbulent flow and heat transfer in a porous-baffled channel. *International Journal of Heat and Mass Transfer*. 46, 771–780. https://doi.org/10.1016/S0017-9310(02)00360-5

Yilmaz, A., Büyükalaca, O., & Yilmaz, T. (2000). Optimum shape and dimensions of ducts for convective heat transfer in laminar flow at constant wall temperature. *International Journal of Heat and Mass Transfer*, 43, 767–775. https://doi.org/10.1016/S0017-9310(99)00189-1